HAL
open science

Onset of power law aftershock decay rates in southern California

C. Narteau, P. Shebalin, M. Holschneider

Onset of power law aftershock decay rates in southern California

C. Narteau

Laboratoire de Dynamique des Fluides Géologiques, Institut de Physique du Globe de Paris, Paris, France

P. Shebalin

International Institute of Earthquake Prediction and Mathematical Geophysics, Moscow, Russia

M. Holschneider

Institutes of Applied and Industrial Mathematics, Universtität Potsdam, Potsdam, Germany

[1] Aftershocks rates seem to follow a power law decay, but the question of the aftershock frequency immediately after an earthquake remains open. We estimate an average aftershock decay rate within one day in southern California by stacking in time different sequences triggered by main shocks ranging in magnitude from 2.5 to 4.5. Then we estimate the time delay before the onset of the power law aftershock decay rate. For the last 20 years, we observe that this time delay suddenly increase after large earthquakes, and slowly decreases at a constant rate during periods of low seismicity. In a band-limited power law model such variations can be explained by different patterns of stress distribution at different stages of the seismic cycle. We conclude that, on regional length scales, the brittle upper crust exhibits a collective behavior reflecting to some extent the proximity of a threshold of fracturing. **Citation:** Narteau, C., P. Shebalin, and M. Holschneider (2005), Onset of power law aftershock decay rates in southern California, *Geophys. Res. Lett.*, *32*, L22312, doi:10.1029/ 2005GL023951.

1. Introduction

[2] A large number of earthquakes in clusters results from perturbation induced by seismic events of larger magnitude. Usually described as aftershocks in the close vicinity of recent ruptures, they have been recently identified as triggered events to take into account longer interaction ranges [*Hill et al.*, 1993]. In order to model the aftershock activity, there is no getting round a power law decay and its most popular form is the modified Omori law (MOL)

$$\Lambda(t) = \frac{K}{(c+t)^p}, \qquad (1)$$

where Λ is the aftershock rate, t is the elapse time from the main shock (i.e., the triggering events), K is a constant, p is the slope of the power law decay, and c is a time shift to avoid a singularity at $t = 0$. This empirical law may be used directly to invert c and p values [*Kisslinger and Jones*, 1991] or recursively applied to all events in an epidemic-type aftershock sequence [*Ogata*, 1988]. In all cases, the parameter c involves a transition from a power law to a slower type of decay as t tends to 0. Such a delay before the

onset of a power law regime is commonly known as the time over which overlapping seismograms and catalog compilers overload prevent the counting of aftershocks. This would imply that earthquakes are strongly under-reported during early parts of aftershock sequences. Nevertheless, visual examination of high-passed seismograms detecting several times more events in the first minutes following main shocks [*Vidale et al.*, 2003, 2004] and statistics on individual sequences [*Narteau et al.*, 2002] show that a transition from a non-power law regime to a power law regime may persist over short times (i.e., $c \neq 0$).

[3] In the last decades, the aftershock decay rate has been put on more solid physical ground as it has been related to fluid migration [*Nur and Booker*, 1972], rate-and-state friction [*Dieterich*, 1994], viscous rheology [*Deng et al.*, 1999] or alternative relaxation mechanisms [*Kisslinger*, 1993]. Following this trend, our objective is to capture the main features of aftershock sequences through a limited number of parameters, which may be correlated with independent data sets [*Narteau et al.*, 2003]. Such an approach complements more empirical law by scrutinizing the evolution of these parameters over different time scales and within different tectonic settings [*Narteau et al.*, 2002]. As an example, we focus here on the onset of the power law regime over short time by analyzing aftershock sequences produced by earthquakes ranging in magnitude from 2.5 to 4.5 in southern California.

2. A Band-Limited Power Law Model of Aftershock Decay Rate

[4] The aftershock zone is modeled by a finite number of independent domains. Just after the main shock at $t = 0$, each of them is intact and initialized to a local overload σ_o which locally combines the state of stress and the state of strength. If the stress exceeds the strength, the overload is positive ($\sigma_o > 0$), the surplus is eliminated through an earthquake, and the domain will produce a unique after-shock. The time of this aftershock depends on the overload according to a Poisson process of rate $\lambda(\sigma_o)$ which determines the characteristic time from an intact state to the rupture. Thus, over the entire population of domains, the aftershock decay rate may be fully described by

$$\Lambda(t) = \int_0^\infty N(\sigma_o, t)\lambda(\sigma_o)d\sigma_o. \qquad (2)$$
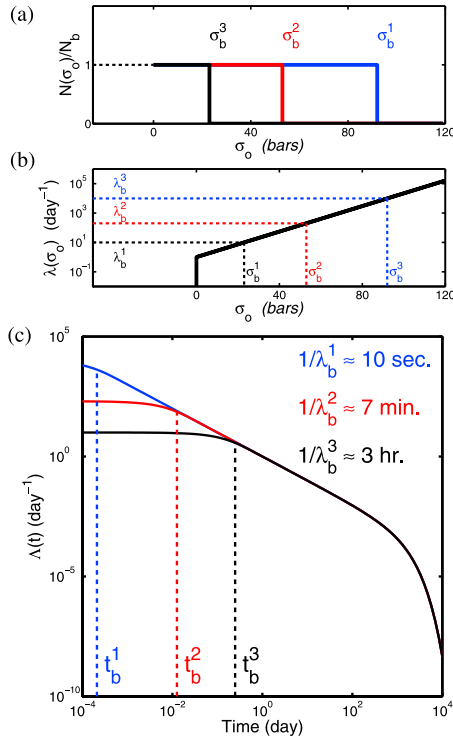
Figure 1. Relationships between the upper bound on the overload distribution, the characteristic aftershock decay rate λ_b and the time delay before the onset of the power law aftershock decay rate. (a) Different overload distributions: $N(\sigma_o) = N_b$ for $0 \leq \sigma_o < \sigma_b^i$, $N(\sigma_o) = 0$ else. (b) The rate function: $\lambda(\sigma_o) = \lambda_a \exp(\sigma_0/\sigma_a)$ for $\sigma_o > 0$, $\lambda(\sigma_o) = 0$ else. (c) The aftershock decay rate. We arbitrarily choose $\lambda_a = 1$ yr^{-1}, $\sigma_a = 10$ *bars* and $\sigma_b^{\{1,2,3\}} = \{23, 53, 92\}$.

[5] *Narteau et al.* [2002] showed that different functions $N(\sigma_o)$ and $\lambda(\sigma_o)$ can be integrated in a single expression

$$\Lambda(t) = \frac{A(\gamma(q, \lambda_b t) - \gamma(q, \lambda_a t))}{t^q}, \qquad (3)$$

where $\gamma(\rho, x) = \int_0^x \tau^{\rho-1} \exp(-\tau) \, d\tau$, is the incomplete Gamma function, A is a constant, and λ_b and λ_a are two characteristic aftershock rates. $\lambda_b = \lambda(\sigma_b)$ corresponds to an upper bound on the overload distribution ($N(\sigma_o > \sigma_b) = 0$, Figure 1a); $\lambda_a = \lambda(0)$ corresponds to a limit of crack growth (Figure 1b). This truncation of the overload distribution at high stress and this threshold of fracturing at low stress follow from the requirement to avoid stress singularities and infinite healing times respectively.

[6] This model appears to give a successful description of the phenomenology of aftershock decay rates investigated all over the world for two reasons. First, power law decay rates with slopes of $q > 1$, $q = 1$ [*Scholz*, 1968] and $q < 1$ emerge from different combinations of overload distributions and rate functions *Narteau et al.* [2002, Figure 1]. Second and more importantly for our immediate concerns, the power law aftershock decay rate is limited by a linear decay over short times and a exponential decay over long times. These temporal limits have already been observed and included in other formula [*Utsu et al.*, 1995], but

equation (3) seems to capture better the transition from one regime to another in a vast majority of cases [*Narteau et al.*, 2002, 2003].

[7] Here, we focus on the transition from a linear decay to a power law decay over short time. In the band-limited power law model (LPL), the onset of the power law aftershock decay rate is delayed according to a decreasing magnitude of the zones of highest overload. For $q = 1$, Figure 1 shows how this time delay is related to the σ_b-value via the characteristic aftershock rate λ_b. Finally, assuming $q = p = 1$ and $\lambda_a \to 0$ in equations (1) and (3), it is possible to show that at $t = 0$

$$c = \frac{K}{A\lambda_b}. \qquad (4)$$

Such a relationship gives a physical interpretation to the parameter c of the MOL. Then, the evolution of the c and λ_b values provide a possible indicator of long-term changes of the state of stress within the brittle upper crust.
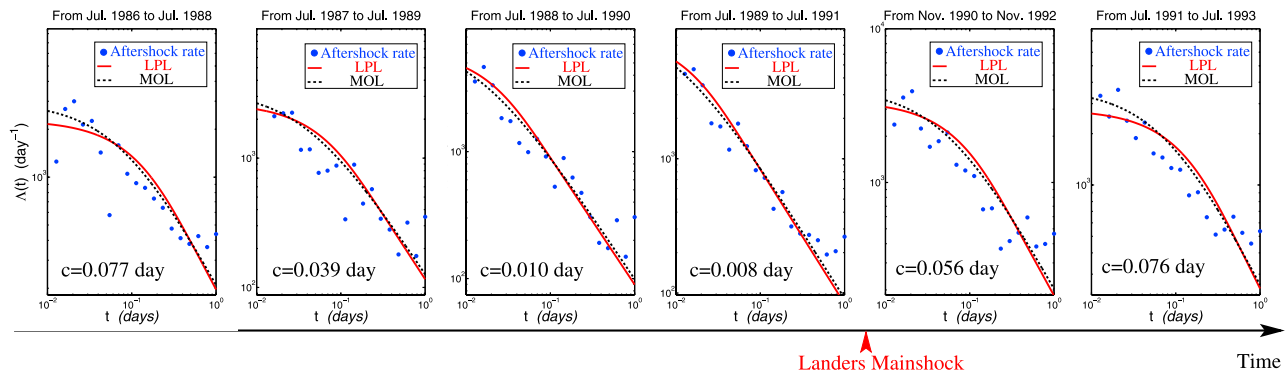
3. Average Aftershock Decay Rate Within the First Day

[8] From the U.S. Advanced National Seismic System (ANSS) composite catalog, we analyze southern California earthquakes located between 31° and 35°N and 240° and 246°E. Main shocks in the magnitude range $2.5 < M < 4.5$ are selected according to *Gardner and Knopoff* [1974] in order to reduce the duration of possible artifacts associated with saturated seismograms. Thus, for example, all earthquake are disregarded during 100 days after a $M = 5$ earthquake within a 40 km radius circle centered at its epicenter. In addition, events preceding over 10 days an earthquake of a magnitude greater or equal at a distance shorter than 50 km are eliminated as potential foreshocks. For all the remaining events, we record their aftershock sequences within 1 day and a 40 km diameter circle. From the main shock list, short term catalogs are generated using a sliding window of 2 years with a time step of two months. Then, for each of these catalogs, we stack the corresponding aftershock sequences by sorting events according to the time interval from their respective main shock. Finally, we end up with a bimonthly average aftershock decay rate over one day and we investigate the onset of the power law regime.

[9] The parameters $\{K, c, p\}$ in equation (1) and the parameters $\{A, q, \lambda_a, \lambda_b\}$ in equation (3) are estimated from observed aftershock sequences using the method of maximum likelihood. For a sequence with N aftershocks occurring at time t_j, $j \in [1, \ldots, N]$ within a $[t_1, t_2]$ time interval, the maximum likelihood function for equations (1) and (3) is

$$L = \exp\left(-\int_{t_1}^{t_2} \Lambda(t)dt\right) \prod_{i=1}^{N} \Lambda(t_i).$$

Parameters are estimated via a method of continuous minimization by simulated annealing [*Press et al.*, 1992],

Figure 2. The average aftershock decay rate within the first day for six periods of time distributed before and after the Landers main shock. Lines represent the best fits provided by the LPL (solid) and the MOL (dashed).

which is more likely to converge to the global maximum, rather than hitting a local one by accident. Practically, we consider $p = q = 1$ and $\lambda_a \rightarrow 0$ (Figures 1 and 2) in order to facilitate the evaluation of c-values and λ_b-values (see equation (4)) as well as the comparison between each of these parameters over different time periods.

4. Onset of the Power Law Regime in Southern California

[10] Before and after the Landers main shock (28/06/1992, 34° 13′N, 243° 32′E), Figure 2 shows the average aftershock decay rates over six different periods of time and the best fit provided by equations (1) and (3). There is a faster onset of the power law decay as the Landers main shock is approached and a sudden transition to a slower onset just after this event. In addition, despite the relationship between c and λ_b, it is possible to verify that the LPL and the MOL does not behave identically. Then, without fixed parameter, we compare these models by calculating ΔAIC values the difference between their Akaike information criterion (AIC = $2n_p - 2 \max\{\ln(L)\}$, where n_p is the number of parameter for a given model). For all time periods since 1985, in 80% of cases, Δ AIC = $\text{AIC}_{\text{LPL}} - \text{AIC}_{\text{MOL}} < -2$ and the LPL fits the data better than the MOL despite an additional parameter.

[11] For the last 20 years, Figure 3 shows large earthquakes and the Benioff strain (square root of the seismic energy) accumulated over the moving time window in southern California and within 3 circles of 50 km radius centered on the Landers, Northridge (17/01/1994, 34 12.8′N, 241° 27.8′E) and Hector Mine (16/10/1999, 34° 13′N, 243° 34′E) hypocenters. Within the same areas, if $N > 40$ the λ_b-value is displayed. The evolution of λ_b is not random and the time delay before the onset of the power law aftershock decay rate varies over two orders of magnitude from 7 min to 12 hours. The λ_b-value variations are asymmetric: short periods of rapid decrease are compensated by long periods of slow and gradual increase. Moreover, over more than 20 *years*, increase rates within different zones are almost constant before an upper limit of the λ_b-value for which aftershocks remain undetectable (i.e., $c < 0.005$ day).

[12] When comparing the evolution of the λ_b-value with the seismicity and the Benioff strain two patterns dominate in all cases: (1) The λ_b-value increases at a constant rate
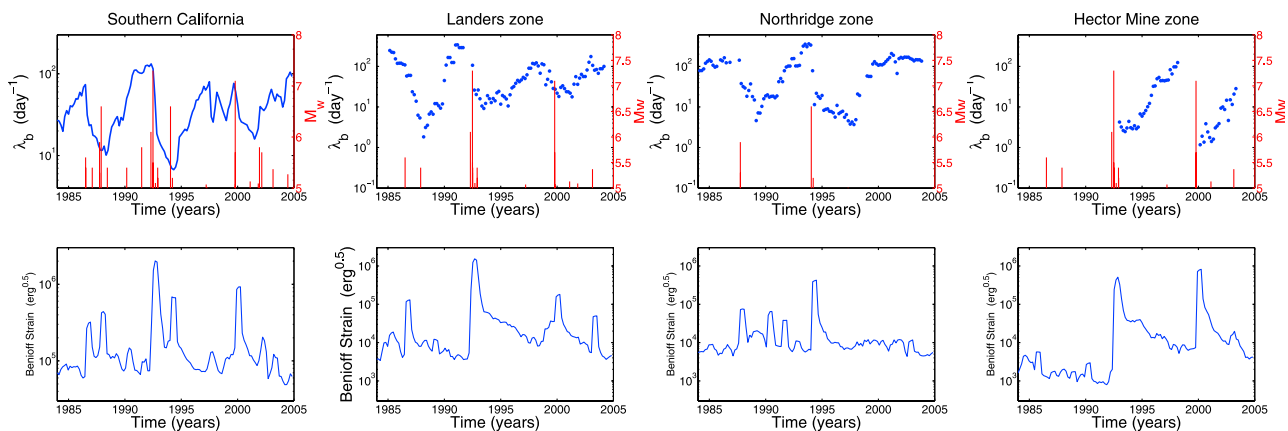
Figure 3. Large earthquakes and evolution of the λ_b-value and of the Benioff strain accumulated over the moving time window in southern California, as well as in the Landers, Northridge, and Hector Mine zones. The λ_b-value is obtained from the best fit provided by the LPL (see Figure 2).
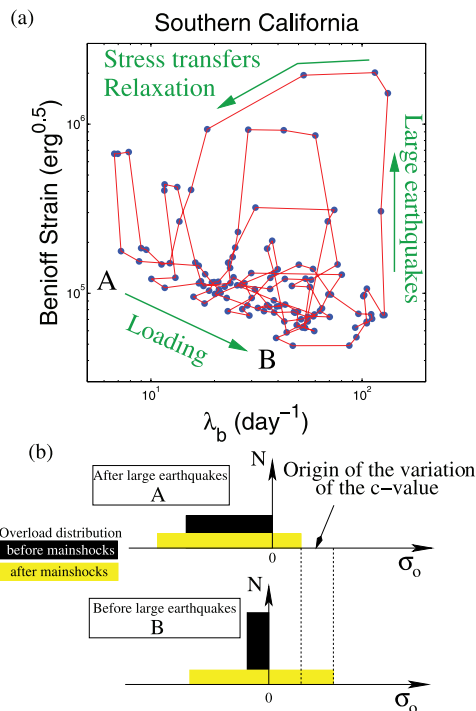
Figure 4. (a) The relationship between the λ_b value and the Benioff strain accumulated over the moving time window. The time evolution is given by the arrows. (b) Schematic representation of the overload distribution at two points in time, before and after a strong earthquake (see text). Dashed lines indicated the upper bounds of the overload distribution.

[15] In the framework of the LPL, the evolution of the λ_b-value indicates that the upper bound of the overload distribution is not constant over a time period of 20 years (Figure 1). Instead, it exhibits an asymmetry which may be related to the seismic cycle picture. Figure 4a shows the relationship between the evolution of λ_b and the evolution of the Benioff strain accumulated over the moving time window. Not surprisingly, a fairly consistent shape emerges from the patterns observed in Figure 3.

[16] 1. The gradual increase of the λ_b-value reflects the loading process during periods of low seismicity. As the stress is building up between large earthquakes, the distribution of overload concentrates just above the threshold of fracturing. Then, perturbations associated with main shocks produce overload distributions with higher upper limits (Figure 4b).

[17] 2. The rapid decrease of the λ_b-value may be associated with the dissipation and the heterogeneities of stress resulting from large earthquakes or from the subsequent stress transfers within the upper crust. It follows a wider overload distribution which is less likely to produce zones of high overload when perturbed by main shocks (Figure 4b).

[18] This work gives a theoretical background for interpreting the behavior of aftershock sequences over short time. The states of stress and strength within fault zones are far more complicated than the overload distributions suggested in Figures 1 and 4b, and they are likely to evolve on short time scales (<1 day). Meanwhile, the systematic occurrence of aftershocks and our statistical procedure may give some insight into the complicated task of estimating the seismic risk in active tectonic zones.

during periods of low seismicity and (2) the λ_b-value collapses when large earthquakes occur.

5. Discussion and Conclusion

[13] Estimations of λ_b and c depend on the number of events via the maximum likelihood function. In order to ensure the statistical significance of our results we consider only sequences with $N > 40$. As the λ_b-value increases with a decreasing seismicity, a small number of aftershocks stacked in time does not seem to be a problem for evaluating the onset of the power law regime over short time. Therefore, low λ_b-value can not be attributed to a lack of events. On the other hand, it is still impossible to analyze time delay shorter than 0.005 day because of a saturation mechanism on seismograms (i.e., $\lambda_b < 300$ day^{-1}).

[14] Here, only small magnitude earthquakes are taken into account and the λ_b-value is averaged over two years within zones that incorporate different faults with different mechanisms. Then, we focus on global properties rather than on local variable. As a consequence, the evolution of the λ_b-value demonstrates some collective behavior on two length scales, the southern California length scale and a regional length scale of approximately 100 km [*Wiemer and Katsumata*, 1999].

References

Deng, J., K. Hudnut, M. Gurnis, and E. Hauksson (1999), Stress loading from viscous flow in the lower crust and triggering of aftershocks following the 1994 Northridge, California, Earthquake, *Geophys. Res. Lett.*, *26*, 3209–3212.

Dieterich, J. (1994), A constitutive law for rate of earthquake production and its application to earthquake clustering, *J. Geophys. Res.*, *99*, 2601–2618.

Gardner, J., and L. Knopoff (1974), Is the sequence of earthquakes in southern California with aftershocks removed poissonian?, *Bull. Seismol. Soc. Am.*, *5*, 1363–1367.

Hill, D., et al. (1993), Seismicity remotely triggered by the magnitude 7.3 Landers, California, earthquake, *Science*, *260*, 1617–1623.

Kisslinger, C. (1993), The stretched exponential function as an alternative model for aftershock decay rate, *J. Geophys. Res.*, *98*, 2271–2281.

Kisslinger, C., and L. Jones (1991), Properties of aftershocks in southern California, *J. Geophys. Res.*, *96*, 11,947–11,958.

Narteau, C., P. Shebalin, and M. Holschneider (2002), Temporal limits of the power law aftershock decay rate, *J. Geophys. Res.*, *107*(B12), 2359, doi:10.1029/2002JB001868.

Narteau, C., P. Shebalin, S. Hainzl, G. Zller, and M. Holschneider (2003), Emergence of a band-limited power law in the aftershock decay rate of a slider-block model, *Geophys. Res. Lett.*, *30*(11), 1568, doi:10.1029/2003GL017110.

Nur, A., and J. Booker (1972), Aftershocks caused by pore fluid flow?, *Science*, *175*, 885–887.

Ogata, Y. (1988), Statistical models for earthquake occurence and residual analysis for point process, *J. Am. Stat. Assoc.*, *83*, 9–27.

Press, W. H., S. A. Teulosky, W. T. Vetterling, and B. P. Flannery (1992), *Numerical Recipes in C*, Cambridge Univ. Press, New York.

Scholz, C. (1968), Microfractures, aftershocks, and seismicity, *Bull. Seismol. Soc. Am.*, *58*, 1117–1130.

Utsu, T., Y. Ogata, and R. Matsu'ura (1995), The centenary of the Omori formula for a decay law of aftershocks activity, *J. Phys. Earth*, *43*, 1–33.

Vidale, J. E., E. S. Cochran, H. Kanamori, and W. Clayton (2003), After the lightning and before the thunder; non-Omori behavior of early aftershocks?, *Eos Trans. AGU*, *84*(46), Fall Meet. Suppl., Abstract S31A-08.

Vidale, J. E., Z. Peng, and M. Ishii (2004), Anomalous aftershock decay rates in the first hundred seconds revealed from the Hi-net borehole data, *Eos Trans. AGU*, *84*(46), Fall Meet. Suppl., Abstract S51C-0170X.

Wiemer, S., and K. Katsumata (1999), Spatial variability of seismicity parameters in aftershock zones, *J. Geophys. Res.*, *104*, 13,135–13,151.

————————————

M. Holschneider, Institutes of Applied and Industrial Mathematics, Universtität Potsdam, POB 601553, D-14115 Potsdam, Germany. (hols@math.uni-potsdam.de)

C. Narteau, Laboratoire de Dynamique des Fluides Géologiques, Institut de Physique du Globe de Paris, F-75252, Paris Cedex 05, France. (narteau@ipgp.jussieu.fr)

P. Shebalin, International Institute of Earthquake Prediction Theory and Mathematical Geophysics, Warshavskoye shosse, 79, korp 2, Moscow 113556, Russia. (shebalin@mitp.ru)